Full Paper

Characterization of Aluminum Powders: II. Aluminum Nanopowders Passivated by Non-Inert Coatings

Alexander Gromov*, Alexander Ilyin

Tomsk Polytechnic University, 30, Lenin Str., Tomsk, 634050 (Russia)

Ulrich Förter-Barth

Fraunhofer Institute for Chemical Technology, Joseph-von-Fraunhofer Str. 7, 76327 Pfinztal (Germany)

Ulrich Teipel

University of Applied Sciences, Particle Technology, Wassertorstr. 10, 90489 Nürnberg (Germany)
DOI: 10.1002/prep.200600055

Abstract

Results of DTA-TG investigation and chemical analysis of electro-exploded aluminum nanopowders, passivated and/or coated with the non-inert reagents: nitrocellulose (NC), oleic acid ($C_{17}H_{33}COOH$) and stearic acid ($C_{17}H_{35}COOH$), which were suspended in kerosene and ethanol, amorphous boron, nickel, fluoropolymer, ethanol and air (for comparison), are discussed. Surface protection of aluminum nanopowders by coatings of different origin results in significant advantages in the energetic properties of the powders. Aluminum nanopowders with a protecting surface show increased stability to oxidation in nitrogen, air and in water during storage period. On the basis of the experimental results, a diagram of the formation and stabilization of the coatings is proposed. The kinetics of the interaction of aluminum nanopowders with nitrogen, air and water is discussed. Recommendations concerning the efficiency of non-inert reagent passivation are proposed on the basis of comprehensive analysis of the experimental data.

Keywords: Aluminum Nanoparticle, Passivation, Non-Inert Coatings, TEM, SEM, DTA-DSC-TG

Introduction

Since the first part of this study was published [1], aluminum nanopowders (ANPs), produced by the electrical explosion of wires (EEW) method, have become the industrial product with a growing market [2]. In recent time, the number of publications, devoted to ANPs, extremely increased [3–5]. This work is aimed to make ANPs closer to application through comprehensive study of their properties. EEW-ANP named ALEX and its analogues have been widely studied as promising components of propellants, mainly. In the case of explosives and pyrotechnics, the effect is not so obvious [2, 5]. Summarizing the last literary data concerning the advantages of ANPs, it is noticeable that the most promising properties of ANPs, predicted by G. V. Ivanov almost 10 years ago [6], are realized in ANP-containing propellants:

1. The temperature of oxidation onset for ANPs is 100–200 °C lower than the aluminum melting point (660 °C); as a result, it is closer to the decomposition temperature for modern oxidizers [7].
2. The powders are stable and not self-aggregative and can be stored in air at room temperature for one or two years, at least [8].
3. The burning rate significantly increases and the burning rate exponent decreases by 20–30% by adding ANPs instead of micron-sized powders in propellants of different types [5].
4. ANPs are ignited and burn inside a very close zone to the propellant burning surface which results in reducing two-phase losses by combustion. At the same time, *Isp* rises and particles burn entirely [9].

On the other hand, the most important problem of the usage of ANPs is the dependence of their properties on the characteristics of their production. Moreover, the EEW-powders, produced by different companies, sometimes have non-reproducible properties; the most negative one is their different stability to oxidation in air, i.e., some ANP samples loose their metal content very fast when stored in air [10]. Mainly, it is due to atmospheric moisture (H_2O), which is more reactive than other air components – O_2, N_2 and CO_2 [11]. Most of the physical properties of EEW-powders can be affected by several parameters, i.e. electrical parameters of powder production (entered energy (E/E_s) and the rate of energy entered into the wire ($R_{E/Es}$), voltage (U), capacity (C) and inductivity (L) of the electric circuit, explosion frequency (f), gas atmosphere in the explosion chamber (Ar,

* Corresponding author; e-mail: gromov@tpu.ru

$Ar + N_2$, $Ar + H_2$ etc.), wire composition and diameter, passivation conditions (gas or liquid passivation reagents, their concentration, solvent used etc.) [12]. Unfortunately, we cannot vary technological parameters within a wide range of values because they mainly depend on the type of machine used for the production of the nanopowders. For commercial and scientific purposes, the majority of producers currently use "machines of the 4th generation" UDP-4 and their analogues, constructed and developed in Tomsk, Russia basically. In the frame of this study some drawbacks for the machine UDP-4 turned out, e.g. the size distribution and the agglomeration degree of the Al particles are practically independent from the electrical regime and wire diameter. Non-passivated ANPs immediately self-ignite if exposed to air, making passivation essential. The majority of commercially available ANPs are passivated by inert oxide layers, consisting of amorphous or crystalline Al_2O_3 [13]. The mechanism of oxide layer formation on metals is widely studied [14]. In fact, the process of oxide layer formation on the surface of nanoparticles upon slow oxidation in air should be called "passivation-up-to-self-saturation". Why the oxidation process stops at a certain thickness of the oxide layer is a topic for further investigation. The structure of such self-saturated oxide layers on Al nanoparticles, produced by EEW, was studied in [15]. A hypothesis of the formation of an electric double layer [16], which is typical for colloidal systems, with additional capacity on the 'metal – oxide' interface of particles has been proposed for the explanation of the relatively high metal content (85 – 90 wt.%) in EEW particles passivated by air [17]. But, the experimental approaches for the maximal metal storage in Al particles and the chemical analysis of the processes, occurring during the particle passivation by different substances, should be developed. Analyzing ANP as a component of energetic compositions [18], we conclude that three main tasks should be solved for the improvement of the properties of ANPs:

1. Increasing the metal content in the powder, i.e. reaching a value comparable to micron-sized powder (95 – 98 wt.% of metal Al).
2. Searching the coating reagents most compatible with recently used propellant binders because ANPs in high concentration extremely increase the propellant viscosity [19].
3. Applied coatings must protect particles from oxidation when stored in air and in propellant binders, but should have no effect on the burning properties of the particles.

The effort of the ANP-with-advanced-properties production is discussed in this work. In several recent studies, non-oxide layers for the passivation of Al nanoparticles have been applied [4, 20], but the metal content was significantly decreased after such treating. In the present work, powders were prepared by EEW method and passivated by different substances applied on their surface: nickel, fluoropolymer, boron, stearic acid, which was suspended in kerosene and ethanol, oleic acid, ethanol, and nitrocellulose. The technique of coating the particles before they come into contact with air was selected because the coating of preliminary air-passivated particles is useless for the solution of task 1: the oxide layer has already formed on the particles (10 – 20 wt.% of Al_2O_3) and cannot be removed or substituted by any kind of after-passivation treatment. For the purpose of comparing, the following air-passivated powders have been produced: aluminum produced in Ar, in gas mixture ($Ar + 10$ vol.% H_2) and commercially available powder (ALEX). The properties of the produced powders were comprehensively studied by several chemical analyses. Experimental data for the mechanism of passivation and oxidation of ANP-with-advanced-properties have been accumulated and analyzed.

2 Experiment

ANPs were produced in argon atmosphere by using the EEW facilities developed by the High Voltage Research Institute, Tomsk, Russia, which was reported elsewhere [21]. The initial Al wire, used for ANP production, was 0.37 mm in diameter and of 99.8% purity. The rate of wire feeding was about 50 mm/s and the explosions were repeated with a frequency ~1.1 Hz. The optimal electrical parameters, preliminary found, were $E/E_s = 1.4$, $U = 26$ kV, $L = 0.6$ μH for the EEW machine UDP-4G. As criterion for powders with optimum characteristics, the highest specific surface area (S_{sp}) was used: for ANP, produced under selected U, L, E/E_s and passivated by air, maximal $S_{sp} \sim 18$ m^2/g. It should be noted that powders with higher S_{sp} can be obtained under higher E/E_s, but ANP, produced under $E/E_s > 1.8$, is a material with non-stable properties, which gradually chemically reacts with almost all known materials except inert gases, but storage of such ANPs in Ar for 1 – 2 days results in self-sintering of the particles because of the extremely high reactivity of the surface of the particles [22]. After producing 1 – 2 kg of powder, the collector with the powder was removed, and the working cycle was repeated.

While the EEW machine was stopped, the collector with the powder was placed into a separate pressure-tight passivation chamber. The list of samples, studied within this work and their specific surface area (S_{sp}), determined by BET method, as well as the metal aluminum content (C_{Al}) after passivation, measured by modified volumetric analysis [23], and the volume mean particle diameter (a_v) are shown in Table 1. The "Zetasizer 3000" by Malvern Instruments, UK, was used for the determination of the particle size distribution and the volume mean particle diameter (a_v).

Sample **1** (ALEX) with widely studied characteristics [24] has been taken for comparison. Sample **2** was an ALEX analogue produced under optimum EEW regime with the UDP-4G machine. Samples **3** and **4** were obtained from the composite wires Al–Ni and Al–B, respectively [25]. For the production of Sample **5**, Ar gas media in the explosion chamber was doped by 10 vol.% of H_2.

Air-passivation (Samples **2** – **5**) was carried out at the $\vartheta = 30 \pm 2\,^{\circ}$C and $p = 0.11$ MPa argon having an air content of about 0.1 vol.%. These conditions of air-passivation of metal

Table 1. Properties of aluminum nanopowders.

No	Sample code	Initial wire composition	Gas media in explosive chamber	Passivation condition	S_{sp} (BET), m^2/g	a_v, nm	C_{Al}, wt.%
1	ALEX	Al	Ar	Air	11.3	484	86
2	Al (Al_2O_3)	Al	Ar	Air	18.6	553	85
3	Al (Ni)	Al (Ni)	Ar	Air	40.7	237	53
4	Al (B)	Al (B)	Ar	Air	12.0	610	84
5	Al ($Ar + H_2$)	Al	$Ar + 10$ vol.% H_2	Air	9.4	583	92
6	Al (St Ac) ethanol	Al	Ar	Stearic acid in ethanol	12.1	255	74
7	Al (St Ac) kerosene	Al	Ar	Stearic acid in kerosene	7.3	410	79
8	Al (Ol Ac)	Al	Ar	Oleic acid in ethanol	14.3	393	45
9	Al (F)	Al	Ar	Teflon	11.6	284	81
10	Al (Ethanol)	Al	Ar	Ethanol	9.8	246	73
11	Al (NC)	Al	Ar	Nitrocellulose in ethanol	12.6	–	68

Table 2. Elemental and phase composition of aluminum nanopowders.

No	Sample code	Wt. content of elements, % (EDX)			Phase composition (XRD)
		O	Al	Ni	
1	ALEX	10	90	–	Al
2	Al (Al_2O_3)	15	85	–	Al
3	Al (Ni)	22	74	4	Al
4	Al (B)	11	89	–	Al
5	Al ($Ar + H_2$)	9	91	–	Al
6	Al (St Ac) ethanol	15	85	–	Al, traces of Al_4C_3
7	Al (St Ac) kerosene	15	85	–	Al
8	Al (Ol Ac)	18	82	–	Al, traces of Al_4C_3
9	Al (F)	12	88	–	Al
10	Al (Ethanol)			n/a	Al
11	Al (NC)			n/a	Al, traces of Al_2O_3

nanopowders were discussed in a previous paper [17]. The ANP Samples **2** – **5**, Table 1, were completely passivated by an Ar/0.1 vol.% air mixture for 72 hours. The end of the passivation period was determined as the moment when the nanopowder stopped reacting with air, i.e. when the pressure of the gas mixture ($Ar + 0.1$ vol.% air) in the passivation chamber stopped decreasing. At higher concentration of air in the passivation gas mixture, self-heating and powder self-sintering occur.

Samples **6** – **11** were passivated by organic substances in solvents before they came into contact with air:

- 0.1 wt.% stearic acid ($C_{18}H_{36}O_2$) solution in ethanol (C_2H_6O);
- 0.1 wt.% stearic acid solution in kerosene;
- 0.1 wt.% oleic acid ($C_{18}H_{34}O_2$) solution in ethanol;
- 0.1 wt.% fluoropolymer solution;
- 97 wt.% ethanol;
- 0.1 wt.% nitrocellulose solution in ethanol.

Ethanol and kerosene were selected as solvents because they do not interact with ANP. The solution for passivation was added to the fresh powder immediately after production and the powder solution was mechanically stirred for ~2 hours. The temperature was maintained at $30 \pm 5\,^{\circ}C$ in order to avoid self-heating of the powder. The residual solvent was evaporated from the ANPs by vacuum treatment at room temperature.

After the passivation procedure, all powders were stored in an open-to-atmosphere-box for 2 months in order to simulate the conditions close to industrial. The morphology and the compositions of the particles (Table 2) were tested by TEM-EDX (Philips CM 200 FEG), SEM (JEOL 6500 F) and XRD (Rigaku "AX-B"diffractometer) with CuK_α radiation. Since non-oxide passivation coatings were applied on ANPs for usage in "Al–H_2O"and solid rocket propellants, three types of ANP- tests were used: reactivity in air (Table 3), in N_2 (Table 4) and in water (Fig. 5). The kinetics of interaction of the samples with 10 wt.% NaOH water-solution was studied. DTA-DSC-TG (Universal 2.4F TA Instruments) was used for testing the non-isothermal oxidation and nitridation.

3 Results

3.1 Properties of the Powders

The reduction in the specific surface area for Samples **6** – **11**, passivated in solutions (Table 1), probably corresponds to residual solvents on the surface of the particles (low metal content, 45 – 81 wt.%) in comparison to Sample **2**, produced

Table 3. Reactivity parameters of aluminum nanopowders under non-isothermal heating in nitrogen.

No	Sample code	$\Delta_{melt}H$ (Al) (at 660 °C), J/g	$T_{nitrid\ onset}$, °C	$\Delta_{nitrid}H$ (Al), J/g	Weight of coating (gases), %	$+\Delta\ m$ (500 – 1000 °C), %	α*** (500 – 1000 °C), %
2	Al (Al_2O_3)	– 245	749	2740	0	38	76
4	Al (B)	– 287	749	534	3	33**	73
6	Al (StAc) ethanol	– 109	690	584	11	16	38
8	Al (Ol Ac)	– 84	700	230	12	21	86
11	Al (NC)	– 89	553	3940	24*	29**	79

* desorption of coating accompany exo-peak on DTA curve (NC decomposition for Sample **11**)
** up to 900 °C
*** $\alpha(Al \rightarrow AlN) = \dfrac{+\Delta m}{C_{Al} \cdot 0,52} \cdot 100\%$
C_{Al}, % – metal content in the samples (Table 1)

Table 4. Reactivity parameters of aluminum nanopowders (m = 7.5 mg) under non-isothermal heating in air.

No	Sample code	$T_{ox\ onset}$, °C	Weight of coating (gases), %	$+\Delta\ m$ (up to 660 °C), %	$+\Delta\ m$ (up to 1400 °C), %	$\Delta_{ox}H$ (Al), J/g	α* (500 – 1400 °C), %
1	ALEX	558	2	26	68	5465	89
2	Al (Al_2O_3)	563	1	9	20	1884	26
3	Al (Ni)	565	9	13	43	–	88
4	Al (B)	556	2	24	63	6232	84
5	Al ($Ar + H_2$)	545	2	25	75	4730	92
6	Al (St Ac) ethanol	549	5	23	58	5997	88
7	Al (St Ac) kerosene	557	6	27	74	6282	105
8	Al (Ol Ac)	486	10	15	38	4875	95
9	Al (F)	538	6	21	68	5184	94
10	Al (Ethanol)	548	5	23	44	5790	68
11	Al (NC)	520	24	10	24	–	40

* $\alpha(Al \rightarrow Al_2O_3) = \dfrac{+\Delta m}{C_{Al} \cdot 0,89} \cdot 100\%$
C_{Al}, % – metal content in the samples (Table 1)

under the same conditions and passivated by air ("dry" technique). The reduction of C_{Al} is maximal for ANP passivated by oleic acid – down to 45 wt.%. Hence, the coating of particles by organic reagents leads to considerable reduction of the specific metal content in the powder (Table 1). In case of boron, this effect is not so obvious. The term "specific metal content" characterizes the content of metal in the powder, but not in the particle. ALEX has a relatively high metal content, and S_{sp} is comparable to Sample **4** (boron coated).

According to TEM, the concentration of Al inside the particles increases when applying organic coatings (Fig. 1), while the specific metal content is lower for powders passivated by organic substances (Table 1). The content of metal in particles, passivated by oleic acid, is higher than for ANP passivated by air. According to TEM data, particles, passivated by air, are covered with oxide films (thickness of 4 – 8 nm), while particles, passivated by oleic acid (Fig. 1b), do not have a visible oxide layer. Analyzing the image in Fig. 1a, we can observe the beginning of oxide film crystallization, i.e. the critical thickness of the amorphous oxide film is 4 – 5 nm after which crystallization begins. Thus, under selected air-passivation conditions, at a thickness of the oxide layer of 4 – 5 nm, oxidation of the particle surface stops and crystallization of the oxide layer occurs.

SEM results confirm that organic-passivated particles hold on their surface a lot of residual solvents (Fig. 2a): particles are not separated as in the case of "dry" powder (Fig. 2b). The narrowest size distribution and finest particles were found in Sample **3** (Fig. 3a). BET and a_v data from Table 1 do not correlate, probably because of the presence of a small amount of very fine particles, but even a small quantity of very fine particles determines the high value of S_{sp}, (see also Fig. 3b). For all samples, the diameter of the largest particles found was not more than 1 – 2 μm (by TEM, SEM and size distribution analyses).

The results of EDX and XRD study of ANPs are presented in Table 2. All powders contain more than 10 wt.% of oxygen (as oxides) on the particle surface. Traces of aluminum carbide were found by XRD for Samples **6** and **8**, but carbon was not determined by EDX because carbon films were used as object slides for the samples. Boron in Sample **4** was not found, probably because of its low molecular weight, and hence EDX method has low sensitivity towards this element. Traces of crystalline aluminum oxide were only found for the sample Al (NC).

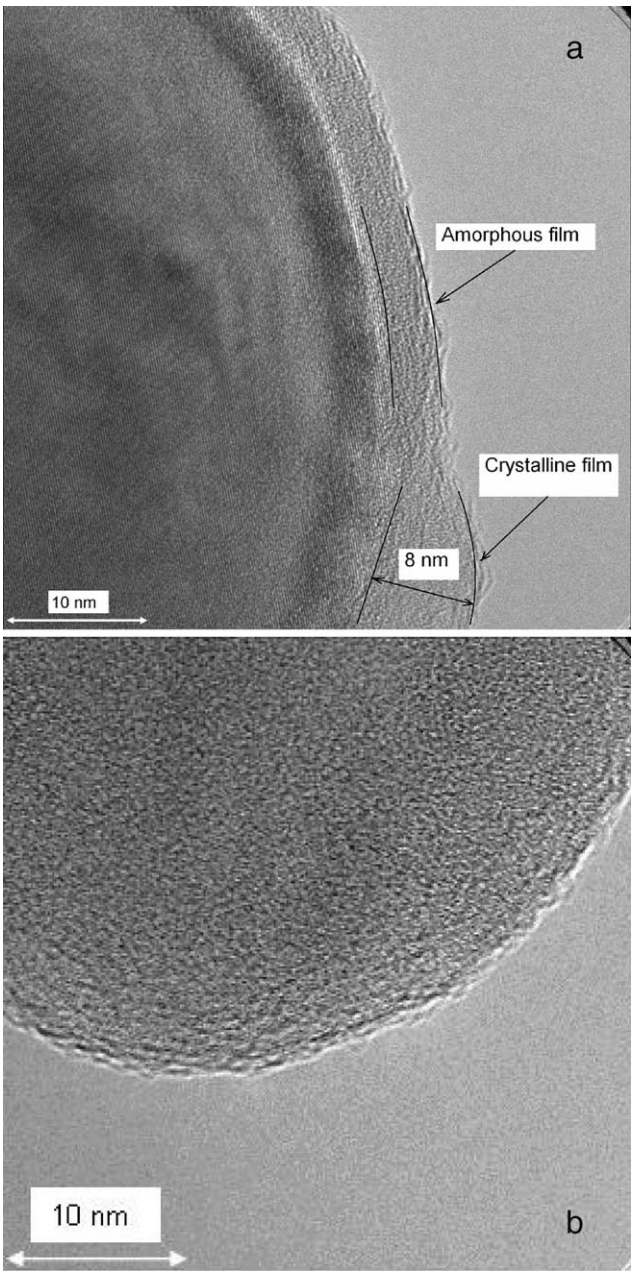

Figure 1. TEM images of ANPs passivated by air (a, Sample **2**) and by oleic acid (b, Sample **8**).

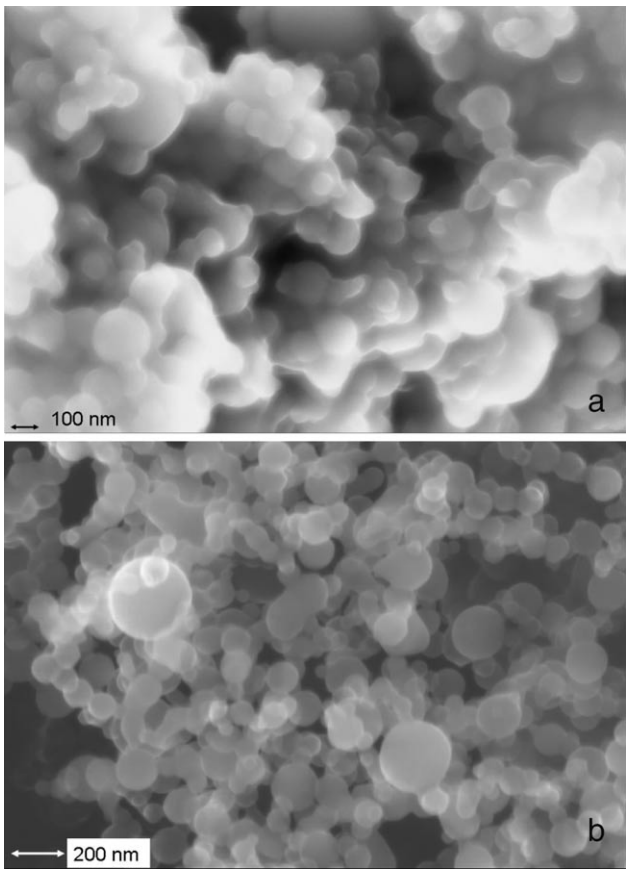

Figure 2. SEM images of ANPs passivated by stearic acid (a, Sample **7**) and by air (b, Sample **2**).

3.2 Non-Isothermal Nitridation and Oxidation

The minimum temperature of nitridation onset ($\vartheta_{nitrid\ onset}$) was for Al (NC) (Sample **11**, Table 3), which was probably caused by the preliminary activation of its surface during the decomposition of NC at 195 °C (Fig. 4). The exothermic effect of nitridation ($\Delta_{nitrid}H$ (Al)) was maximal for the sample Al (NC) (3940 J/g), which could be due to both the simultaneous nitridation of aluminum during the decomposition of residual NC and the nitridation of aluminum as a result of the preliminary activation of the surface. The degree of transformation of Al into AlN was maximum for ANP passivated by oleic acid (Sample **8**, Table 3).

In contrast to nitrogen, the beginning of intensive ANP oxidation in air was below the melting point of aluminum (660 °C). The results of DSC-TG analysis of ANP samples in air are represented in Table 4. The non-isothermal heating was executed with a rate of heating of 10 K/min. The maximum temperature of oxidation onset ($\vartheta_{ox\ onset}$) is characteristic for Sample **3.** Probably, this is caused by the presence of refractory nickel (see Table 2) in the composition of the passivating layer on the particle surface. The $\vartheta_{ox\,onset}$ of the samples, passivated by air, changes in the range of 564 – 545 °C and does not correlate with the dimensional characteristics of the powders and the type of the passivating coating. For Sample **8**, the oxidation begins at 486 °C (much lower than the melting point of aluminum). The adsorbed gas weight of "dry" ANPs (Samples **1** – **5**) does not exceed 2%, with the exception of the nickel-containing sample. The mass of organic coatings (Samples **6** – **11**) is 3 – 4 times higher than for the "dry" Samples **1** – **5.** It should be noted that the full value of the mass of coatings is even higher, since the oxidation processes of coating and interaction "aluminum – coating" simultaneously occur with desorption (see Table 3, where the weight of the coatings is higher for the same samples). The degree of conversion to 1400 °C (last column, Table 4) is relatively high for all samples, except Sample **2.** Apparently, oxide-coated particles degraded very

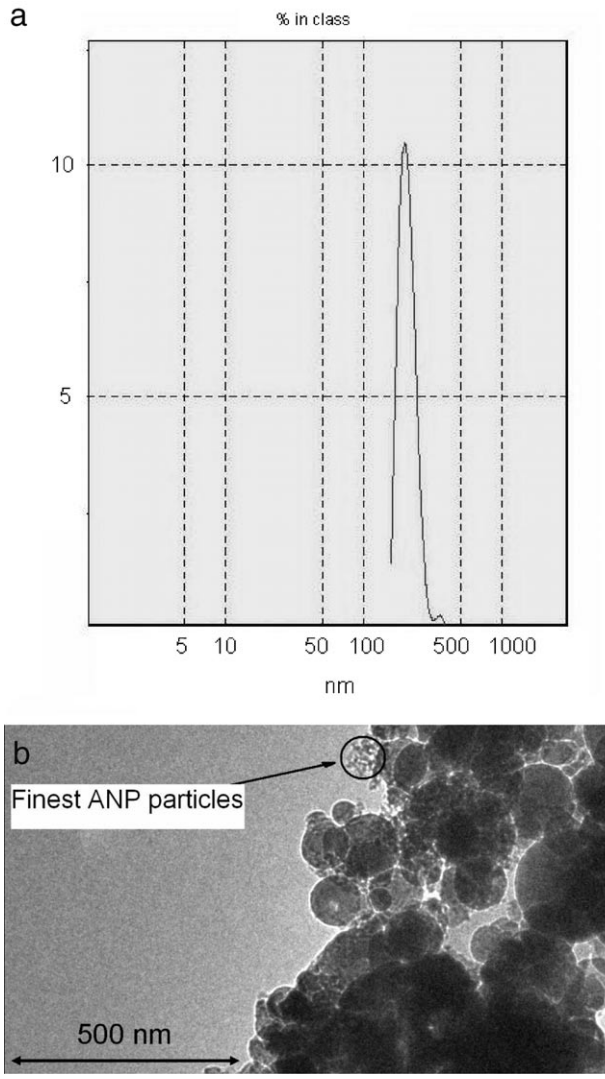

Figure 3. Size distribution (a) and TEM image (b) of ANPs, obtained from the composite wire Al-Ni (Sample **3**), passivated by air.

fast by storage. The value of α of more than 100% for Sample **7** (Table 4) is caused by the oxidation of kerosene covering the surface of the particles.

3.3 Interaction with Water

The kinetics of the interaction of the powders with water was investigated in a 10% NaOH solution at a temperature of 20 °C (Fig. 5). The kinetic curves for all powders have the same character, but Samples **1**, **2** and **5** (Table 1) practically have no induction period, other ANP samples show a good stability in the NaOH solution. Thus, practically each of the organic coating protects the particle surface against oxidation in water better than the oxide ones.

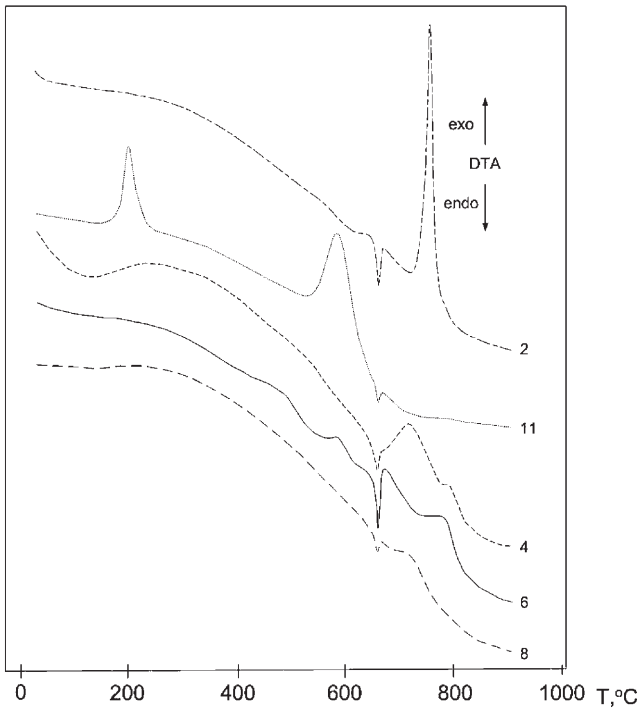

Figure 4. DTA curves for selected samples of ANPs under non-isothermal heating in nitrogen ($m = 4.4$ mg, $v_{heat} = 10$ K/min, etalon α-Al_2O_3). The numbers of the curves correspond to the numbers of the samples in Table 1.

4 Discussion

A comparison of the properties of the studied ANP samples has been made for three groups:

1. ALEX, Al ($Ar + H_2$) and Al (Al_2O_3) powders – air passivated;
2. Al (Ni) and Al (B) powders – passivated by inorganic coatings;
3. Al (St Ac) ethanol, Al (St Ac) kerosene, Al (Ol Ac), Al (F), Al (Ethanol) and Al (NC) powders – passivated by inorganic coatings.

4.1 ALEX, Al ($Ar + H_2$) and Al (Al_2O_3) Powders

According to TEM, ALEX is less agglomerated than Al (Al_2O_3) (Fig. 6) though produced and passivated similarly. The agglomeration of Al particles in the explosive chamber is only determined by the explosion regime and the aerodynamics of the particles in the chamber. The process of agglomeration cannot be controlled at the stage of passivation when particles have already cooled. The specific metal content of ALEX, Al ($Ar + H_2$) and Al (Al_2O_3) is the highest compared to the other powders, but, at the same time, Al ($Ar + H_2$) has S_{sp} half as much as that of Al (Al_2O_3): the explosion in the mixture ($Ar + H_2$) results in the formation of larger particles, but less oxidized (Tables 1 and 2). Additionally, dissolved hydrogen can be a reason for

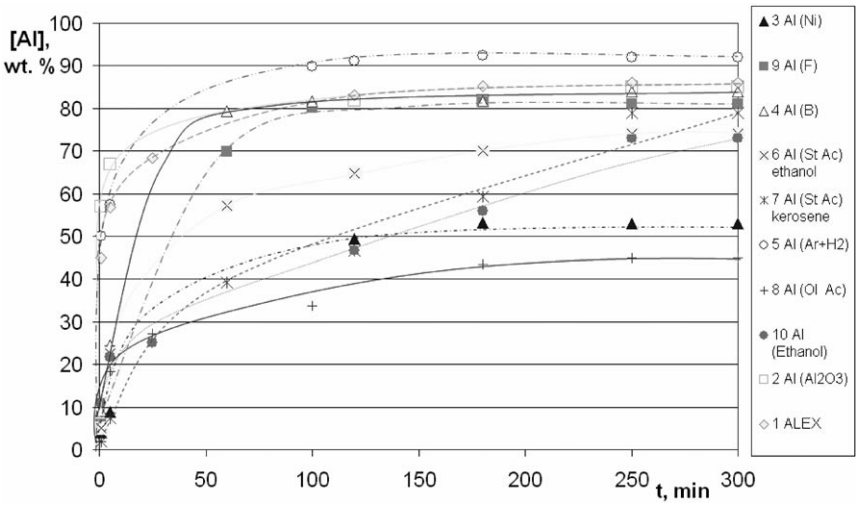

Figure 5. Kinetic curves for aluminum nanopowders with different coatings, interaction with 10 wt.% NaOH water solution. Numbers of samples in Table 1.

the earlier oxidation onset of Al ($Ar + H_2$) compared to ALEX and Al (Al_2O_3) (Table 4).

The DTA-TG curve of Al (Al_2O_3) shows low α compared to ALEX and Al produced in hydrogen-enriched argon. Thus, the powder, produced in Ar and passivated by air, is not stable to oxidation during storage: the metal content significantly decreases during 2 month storage. The reaction of the "dry" powders with water has no induction period (Fig. 5). Hence, the oxide film has low protective properties in water.

4.2 Al (Ni) and Al (B) Powders

The sample Al (Ni) consists of two types of particles (Fig. 3b): a very fine fraction and large particles. 4 wt.% of Ni (Table 2), according to EDX, does not cover the surface of large Al particles, but Ni is separately distributed in a small oxidized fraction. Particle surfaces for this sample are not smooth. Thus, the explosion of Al–Ni composite wires results in the formation of smaller particles (Table 1) compared to Al without coating, but the size of such small particles is less than the border of stability – about 30 nm [26]. The residual non-oxidized Al particles completely react with air at $T < 1000\,^{\circ}C$ (Table 4): Ni does not increase the stability of fine Al particles to oxidation in air.

Boron-stabilized nano-Al [27] is an attractive material for propellants, because boron-coated particles can increase the powder combustion enthalpy. The aluminum content and S_{sp} for this sample are nearly the same as for Sample **1** (ALEX, Table 1), and the degree of conversion up to 1400 °C is not very low (Table 4). Boron-coated powder has also a high value of $\Delta_{ox}H$ in air (Table 4). Boron-coated particles react with water having a very short induction period (few seconds, Fig. 5). Ni-coated particles have low Al metal content determined by reaction with water. It can be caused by the presence of a lot of NiO and a big fraction of very fine oxidized particles.

4.3 Al (St Ac) Ethanol, Al (St Ac) Kerosene, Al (Ol Ac), Al (F), Al (Ethanol) and Al (NC) Powders

Stearic acid and oleic acid have the same effect on the passivation of Al particles – they interact with aluminum. In the case of oleic acid, the interaction with the metal was stronger – C_{Al} decreased to 45 wt.% in Sample **8** (Table 1). It is noticeable that the interaction of Al with stearic acid and oleic acid results in the carbidization of the particle surface (see Table 2). Ethanol without organic acid acts similarly: it decreases the metal content in the powders and does not improve the powder reactivity in air (Table 4). Al (F) and Al (NC) seem to be promising for the use in combustion processes, but the metal content is low. For the majority of organic-coated particles, we did not observe strong organic layers which could protect Al particles from further oxidation. In the case of Al (Ol Ac), the particles contain more oxygen than other samples (Table 2). Moreover, according TEM, organic-coated metal particles have two layers: an organic layer and an internal oxide layer (Fig. 7).

5 Conclusion

Eleven samples, produced under different experimental conditions and stabilized by organic and inorganic substances, have been studied. The most important advantage of non-oxide coated aluminum nanoparticles is their expected higher combustion enthalpy compared to Al_2O_3-passivated Al particles. The drawback of non-oxide coatings is the decreasing of the specific metal content. When calculating the quantity of Al for the preparation of propellant compositions, the content of the coating on the particle

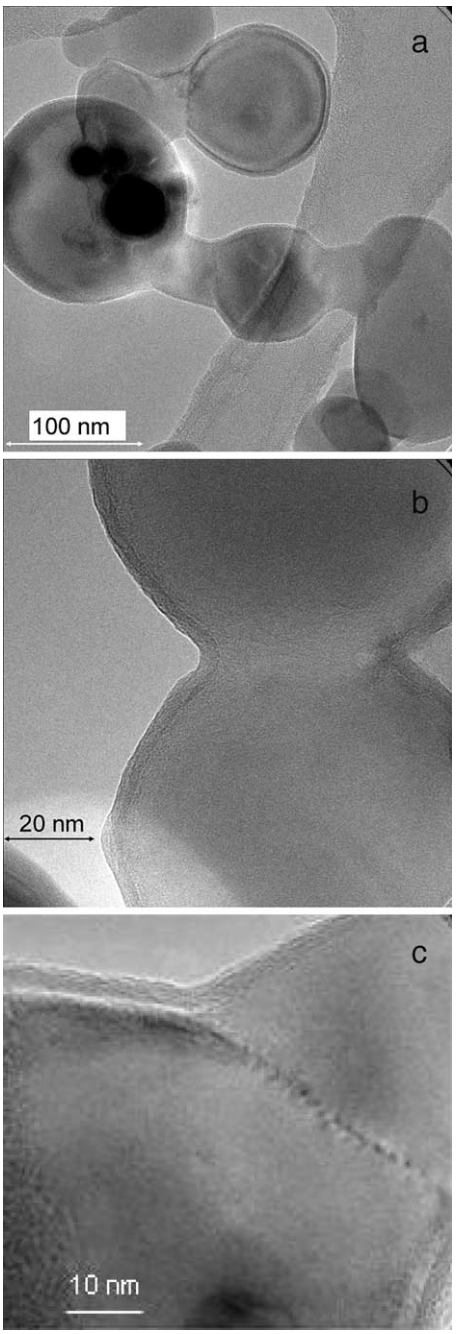

Figure 6. Substructure of agglomerates of ANP particles (Sample **2**) passivated by air: a – necks between particles, b – sintered particles, c – neck substructure.

surface should be taken into account. Among the studied samples, more attention should be paid for three powders: Al ($Ar + H_2$) and Al (B) for solid propellants and Al (St Ac) for "Al-water" propellants. In contrast to micron-sized Ni coated Al powders [28], ANPs, coated by Ni, contain a lot of Ni (lower burning enthalpy) and are more oxidized. Coating of particles by fluoropolymer is also not profitable: fluorine has not been found on the particles and the powder has ordinary characteristics by non-isothermal oxidation in air and in water. For all organic-coated particles, the organic

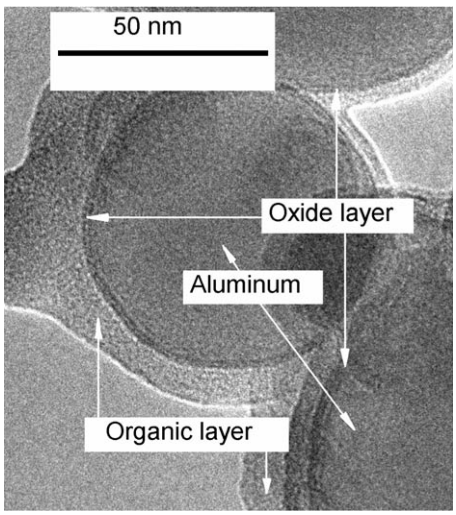

Figure 7. Two-layer coating of organically passivated Al particles.

layer is transparent for oxygen and results in internal oxide layer formation (Fig. 7).

6 References

[1] A. Ilyin, A. Gromov, V. An, F. Faubert, C. de Izarra, A. Espagnacq, L. Brunet, Characterization of Aluminum Powders: I. Parameters of Reactivity of Aluminum Powders, *Propellants, Explos., Pyrotech.* **2002**, *27*, 314.
[2] U. Teipel, *Energetic Materials*, Wiley-VCH, Weinheim **2004.**
[3] N. Eisenreich, H. Fietzek, M. Juez-Lorenzo, V. Kolarik, A. Koleczko, V. Weiser, On the Mechanism of Low Temperature Oxidation for Aluminum Particles down to the Nano-Scale, *Propellants, Explos., Pyrotech.*, **2004**, *29*, 137.
[4] D. E. G. Jones, R. Turcotte, R. C. Fouchard, Q. S. M. Kwok, A.-M. Turcotte, Z. Abdel-Qader, Hazard Characterization of Aluminum Nanopowder Compositions, *Propellants, Explos., Pyrotech.* **2003**, *28*, 120.
[5] Yu. F. Ivanov, M. N. Osmonoliev, V. S. Sedoi, V. A. Arkhipov, S. S. Bondarchuk, A. B. Vorozhtsov, A. G. Korotkikh, V. T. Kuznetsov, Productions of Ultra-Fine Powders and Their Use in High Energetic Compositions, *Propellants, Explos., Pyrotech.* **2003**, *28*, 319.
[6] G. V. Ivanov, F. Tepper, Activated Aluminum as a Stored Energy Source for Propellants, *4th International Symposium on Special Topics in Chemical Propulsion, Challenges in Propellants and Combustion 100 Years after Nobel*, Stockholm, 27 – 31 May **1996.**
[7] H. H. Krause, New Energetic Materials, in U. Teipel (Ed.), *Energetic Materials*, Wiley-VCH, Weinheim **2004**, p. 1.
[8] J. C. Sanchez-Lopez, A. Fernandez, C. F. Conde, A. Conde, C. Morant, J. M. Sanz, The Melting Behavior of Passivated Nanocrystalline Aluminum, *Nanostruct. Mat.* **1996**, *7*, 813.
[9] P. F. Pokhil, A. F. Belyaev, Yu. V. Frolov, V. S. Logachev, A. I. Korotkov, Combustion of Powdered Metals in Active Media, Nauka, Moscow, **1972.** See also FTD-MT-24-551-73 translated from Russian by Foreign Technology Division, Wright Patterson Air Force Base, Ohio, 1973.
[10] A. P. Ilyin, A. A. Gromov, *Ultrafine Aluminum and Boron Combustion*, Tomsk State University Press, **2002**, p. 165 [in Russian].

[11] Q. S. M. Kwok, R. C. Fouchard, A.-M. Turcotte , P. D. Lightfoot, R. Bowes, D. E. G. Jones, Characterization of Aluminum Nanopowder Compositions, *Propellants, Explos., Pyrotech.* **2002**, *27*, 229.
[12] E. I. Azarkevich, A. P. Ilyin, D. V. Tikhonov, G. V. Yablunowskii, Electric Explosion Synthesis of Ultradispersed Powders of Metals, Alloys and Chemical Compounds, *Physics and Chemistry of Materials Treatment* (*Physica i Khimiya Obrabotki Materialov)*, **1997**, *4*, 85 [in Russian].
[13] J. C. Sanchez-Lopez, T. C. Rojas, J. P. Espinos, A. Fernandez, "In Situ" XPS Study of the Oxygen Passivation Process in Vapour-Condensed Nanocrystalline Iron and Cobalt, *Scr. Mater.* **2001**, *44*, 2331.
[14] A. P. Ilyin, A. A. Gromov, G. V. Yablunovskii, Reactivity of Aluminum Powders, *Combustion, Explosion and Shock Waves*, **2001**, 37, *4*, 418.
[15] A. L. Ramaswamy, P. Kaste, Combustion Modifiers for Energetic Materials, *34th Int. Annual Conference of ICT*, Karlsruhe, 24 – 27 June **2003**, p. 21/1.
[16] Z. W. Wang, X. Z. Yi, G. Z. Li, D. R. Guan , A. J. Lou, A Functional Theoretical Approach to the Electrical Double Layer of a Spherical Colloid Particle, *Chem. Phys.* **2001**, *274*, 57.
[17] Y. S. Kwon, A. A. Gromov, A. P. Ilyin, G. H. Rim, Passivation Process for Superfine Aluminum Powders Obtained by Electrical Explosion of Wires, *Appl. Surf. Sci.* **2003**, *211*, 57.
[18] Y. S. Kwon, J. S. Moon, A. P. Ilyin, A. A. Gromov, Estimation of the Reactivity of Aluminum Nanopowders for Energetic Applications, *Combustion Sci. Technol.* **2004**, *176*, 277.
[19] U. Teipel, U. Förter-Barth, Rheology of Nano-Scale Aluminum Suspensions, *Propellants, Explos., Pyrotech.* **2001**, *26*, 268.
[20] A. N. Jigatch, I. O. Leipunsky, M. L. Kuskov, P. A. Pshenchenkov, N. G. Berezkina, M. N. Larichev, V. G. Krasovskii, Synthesis of Coatings on a Surface of Ultrafine Particles of Aluminum, *Chemical Physics* (*Khimicheskaya Fizika*), **2002**, *21*, 72 [in Russian].
[21] Y. S. Kwon, Y. H. Jung, N. A. Yavorovsky, A. P. Ilyin, J. S. Kim, Ultrafine Metal Powders by Wires Electric Explosion Method, *Scr. Mater.* **2001**, *44*, 2247.
[22] A. P. Ilyin, A. A. Gromov, A. A. Reshetov, T. V. Tikhonov, G. V. Yablunowsky, Reactionary Ability of Aluminum Ultrafine Powders in Various Oxidation Processes, *4th Korea – Russia International Symposium on Science and Technology (KORUS 2000)*, Ulsan (South Korea), 27 June – 1 July **2000.**
[23] T. D. Fedotova, O. G. Glotov, V. E. Zarko, Chemical Analysis of Aluminum as a Propellant Ingredient and Determination of Aluminum and Aluminum Nitride in Condensed Combustion Products, *Propellants, Explos., Pyrotech.* **2000**, *25*, 325.
[24] M. M. Mench, K. K. Kuo, C. L. Yeh, Y. C. Lu, Comparison of thermal Behavior of Regular and Ultrafine Aluminum Powders (Alex) Made from Plasma Explosion Process, *Combust. Sci. Technol.* **1998**, *135*, 269.
[25] A. P. Ilyin, Yu. A. Krasnyatov, D. V. Tikhonov: Russian Federation Patent 2139776.
[26] K. J. Klabunde, *Nanoscale Materials in Chemistry*, Wiley-VCH, **2001.**
[27] Y. S. Kwon, A. A. Gromov, A. P. Ilyin, Reactivity of Superfine Aluminum Powders Stabilized by Aluminum Diboride, *Combust. Flame* **2002**, *131*, 349.
[28] A. L. Breiter, V. M. Maltsev, E. I. Popov, Ways for Modification of Powdery Metals for Condensed Systems, *Fiz. Goreniya Vzryva* **1990**, *26*, 97 [in Russian].

List of abbreviations

ALEX	Aluminum explosive (TM);
ANP	Aluminum nanopowder;
a_v	Volume mean particle diameter, nm
C_{Al}	Metal aluminum content, wt.%
DSC	Differential scanning calorimetry;
DTA	Differential thermal analysis;
EDS	Electron diffraction spectroscopy;
E/E_s	Energy entered into the wire, a.u.;
EEW	Electrical explosion of wires;
HTPB	Hydroxy-terminated polybutadiene;
SEM	Scanning electron microscopy;
S_{sp}	Area of the specific surface, m^2/g
TEM	Transmission electron microscopy;
TG	Thermogravimetry;
XRD	X-ray diffraction.

Acknowledgements

This work has been supported by INTAS grant YSF 55-03-671 and Russian President grant 1812.2005.8.

(Received July 19, 2005; Ms 2005/042)

